



ELSEVIER

Journal of Chromatography A, 890 (2000) 81–94

JOURNAL OF
CHROMATOGRAPHY A

www.elsevier.com/locate/chroma

Trapping the monomeric α -helical state during unfolding of coiled-coils by reversed-phase liquid chromatography

Y. Bruce Yu^a, Kurt C. Wagschal^b, Colin T. Mant^b, Robert S. Hodges^{a,b,*}

^aProtein Engineering Network of Centres of Excellence, University of Alberta, Edmonton, Alberta, T6G 2S2, Canada

^bDepartment of Biochemistry and the Medical Research Council of Canada Group in Protein Structure and Function, University of Alberta, Edmonton, Alberta, T6G 2H7, Canada

Abstract

Reversed-phase liquid chromatography (RPLC) offers a unique opportunity to monitor the transition from the native state (N) to the structural intermediate state (I) for proteins whose secondary structure is comprised entirely of amphipathic helices, such as coiled-coils. During RPLC, the hydrophobicity of the stationary phase and mobile phase results in the unfolding of the tertiary/quaternary structure of coiled-coils but retains α -helical secondary structure and thus isolates the I state. A set of five peptides, $\alpha\alpha$ -36, $\beta\beta$ -36, $\alpha\beta$ -36, $\gamma\delta$ -36 and $\omega\omega$ -36, was generated by shuffling guest hydrophobes at equivalent sites in a symmetric host frame. In one of the peptides, $\omega\omega$ -36, all the α -glutamic residues in the host frame were replaced by γ -glutamic residues. $\alpha\alpha$ -36, $\beta\beta$ -36, $\alpha\beta$ -36, $\gamma\delta$ -36 form two-stranded coiled-coils of identical helical content and unfold as a two-state transition during temperature denaturation while the fifth peptide, $\omega\omega$ -36, is a random coil and cannot be induced in to an α -helical structure even in the presence of a helix inducing solvent, 50% trifluoroethanol. By comparing the stability order of the four coiled-coils in the N \rightarrow I transition (measured by RPLC studies) with that in the N \rightarrow D (denatured state) transition (measured by calorimetry), it is concluded that there is a direct correlation between the relative stabilities of these peptides in these two unfolding transitions. This result supports a hierarchical folding mechanism for coiled-coils. © 2000 Elsevier Science B.V. All rights reserved.

Keywords: Protein folding; Protein coiled cells; Proteins; Peptides

1. Introduction

To study the protein folding process, it is imperative to clarify the relationships among the native state (N, the state with both tertiary/quaternary and secondary structure), the structural intermediate state (I, the state with native secondary structure but no tertiary/quaternary structure) and the denatured state (D, the state with neither tertiary/quaternary nor secondary structure) [1–4]. This is hampered by a shortage of techniques to trap the I state. Previous

studies have shown that reversed-phase liquid chromatography (RPLC) can, on the one hand, disrupt protein tertiary/quaternary structures, and on the other hand, induce and stabilize helical structure in amphipathic peptides [5–12]. Therefore, for proteins whose secondary structure is entirely comprised of amphipathic helices, such as coiled-coils, RPLC may offer a unique opportunity to trap the I state and to investigate the N \rightarrow I transition. We selected the two-stranded α -helical coiled-coil because it provides the simplest case of subunit interactions, that is, two interacting amphipathic α -helices. A two-stranded coiled-coil is comprised of two right-handed α -helices wrapping around each other to form a slightly

*Corresponding author. Fax: +1-780-492-1473.

E-mail address: robert.hodges@ualberta.ca (R.S. Hodges).

left-handed super-helix [13]. The hydrophobic surface from each amphipathic α -helix forms an interhelical hydrophobic core which is largely shielded from solvent [14]. Sequentially, each polypeptide chain contains a 3~4 or 4~3 hydrophobic repeat where each heptad is denoted as *abcdefg* and where positions *a* and *d* are non-polar [15]. For recent reviews on α -helical protein assembly motifs and coiled-coils see Refs. [16–20]. These structural and sequential features make it an ideal candidate to explore the possibility of using RPLC to monitor the N→I transition.

2. Experimental

2.1. Materials

Biograde grade trifluoroacetic acid (TFA) was obtained from Halocarbon Products (River Edge, NJ, USA.). Acetonitrile was obtained from EM Science (Gibbstown, NJ, USA.).

2.2. Peptide synthesis, purification and modification

Peptides were synthesized either manually or on an Applied Biosystems peptide synthesizer Model 430 (Foster City, CA, USA), using *tert*-butyloxycarbonyl (*t*-Boc) chemistry on 4-methylbenzhydrylamine resin. α -Glutamyl residues (E) were introduced by using N- α -*t*-Boc-L-glutamic acid γ -benzyl ester while γ -glutamyl residues (ϵ) were introduced into the polypeptide chain by using N- α -*t*-Boc-L-glutamic acid α -benzyl ester. Crude peptides were purified by preparative RPLC, using standard protocols described previously [5–7]. Disulfide-bridged homodimers were formed by air oxidation of the polypeptide containing cysteine in 100 mM NH_4HCO_3 at pH 8.0. For the formation of the heterodimers, one polypeptide was derivatized with 2,2'-dithiobis(5-nitropyridine) (DTNP) and reacted with the other polypeptide containing cysteine [21,22]. Carboxamidomethylation of the cysteine residue in the peptides was carried out at pH 8–8.5 using iodoacetamide [23,24]. Authenticity of the peptides was verified by electrospray mass spectrometry on a VG Quattro triple quadrupole mass

spectrometer (VG BioTech, Altrincham, UK). All products were within 2 Da of calculated molecular mass (9096 for the crosslinked peptides and 4607 for the carboxamidomethylated peptides).

2.3. HPLC columns, run conditions and instrument

Analytical runs were carried out on a Zorbax 300SB-C₈ column (150 mm×2.1mm I.D., 5 μm particle size, 300 Å pore size) using an HP1100 chromatograph system, both from Hewlett-Packard (Avondale, PA, USA). A linear AB gradient elution (1% B/min) was employed with eluent A being 0.05% TFA in water and B being 0.05% TFA in acetonitrile. The flow-rate was 0.4 ml/min. Runs were carried out at 5°C to 80°C in 5°C increments from run to run. The temperature control was afforded by the HP1100 system. Peptides RC11 and RC30 were included in every HPLC run as internal random coil standards to standardize retention behavior. The corrected retention of a sample peptide, $t_{\text{R, corrected}}$, is defined as:

$$t_{\text{R, corrected}} = t_{\text{R}}(\text{peptide}) - t_{\text{R}}(\text{random coil}),$$

where $t_{\text{R}}(\text{peptide})$ is the experimental retention time of the sample peptide while $t_{\text{R}}(\text{random coil})$ is the retention time of a random coil peptide which has the same amino acid composition and neighboring residue pairs as the sample peptide.

2.4. Circular dichroism (CD) spectroscopy

Ellipticity of the peptides was measured on a Jasco 500C spectropolarimeter (Jasco, Easton, MD, USA.). The cell was maintained at 25°C with a Lauda EMS circulating water bath (Westbury, NY, USA.). The spectropolarimeter was calibrated using *d*-10-camphorsulfonate. The samples were dialyzed extensively in H_3PO_4 - H_2O , pH 2.0, before measurements. The concentrations of peptide samples were determined by their UV absorption spectra with light scattering corrected in 5–6 M guanidinium hydrochloride at pH 6.5. The extinction coefficients used for the crosslinked peptides and the carboxamidomethylated peptides are 5945 $\text{M}^{-1}\cdot\text{cm}^{-1}$ and 2900 $\text{M}^{-1}\cdot\text{cm}^{-1}$ at 275 nm, respectively, calculated from their amino acid compositions [25].

2.5. Analytical ultracentrifugation

Sedimentation equilibrium studies were performed on a Beckman XLI analytical ultracentrifuge equipped with Rayleigh interference optics. Each sample was loaded at three different concentrations using a 6-sector charcoal-filled epon cell and run at three speeds: 26k, 30k and 34k rpm. The radial equilibrium concentrations were analyzed using the program NONLIN. The entire concentration ranges are 0.10–0.95 mg/ml for α 36-CM (where CM = carboxamidomethyl) and 0.08–1.05 mg/ml for β 36-CM. The data were best described by a single species model for a dimer with excellent fit as indicated by the square root of variance of less than 0.02.

3. Results and discussion

3.1. A working hypothesis

By comparing the retention behavior and CD spectra of amphipathic and non-amphipathic peptides of different chain lengths, it has been demonstrated previously that the quaternary/tertiary structures of highly stable non-crosslinked coiled-coils are disrupted during RPLC. Each amphipathic polypeptide chain of the coiled-coil binds to the stationary phase as a single-stranded α -helix [5–7]. Furthermore, the organic co-solvent of the mobile phase has the same effect, i.e., the amphipathic peptides exist in the mobile phase also as single-stranded α -helices, rather than a two-stranded coiled-coil, upon elution. It was shown later by *in situ* CD spectroscopy measurements that the conformation of bound amphipathic peptides on RPLC stationary phase ligands is indeed α -helical [11]. Therefore, for the folding/unfolding process of coiled-coils, the RPLC stationary phase alkyl ligands alter the equilibrium between the N state and the I state by trapping the latter through hydrophobic interactions. This is illustrated schematically in Fig. 1. Thus, RPLC offers a means to investigate the N \rightarrow I transition. Understanding the unfolding of multimeric proteins is complicated by the monomer–oligomer equilibrium. Thus, cross-linked coiled-coils are advantageous over non-cross-linked ones because the issue of concentration

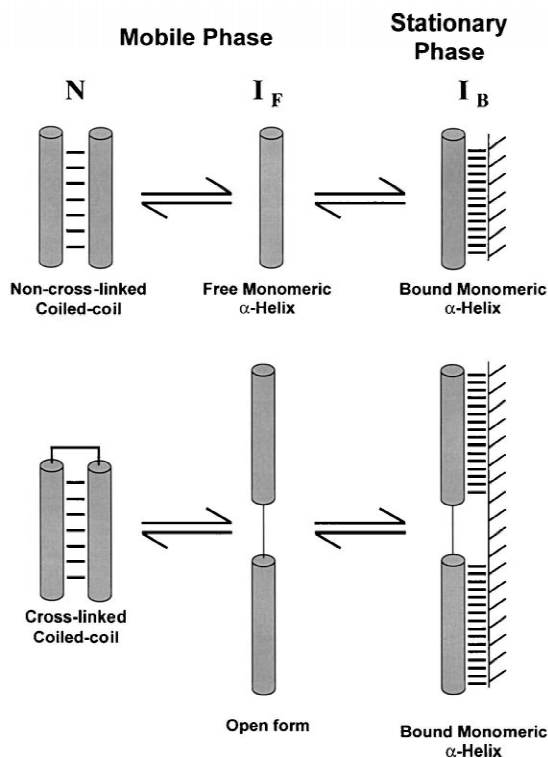


Fig. 1. Schematic diagram illustrating the structural status of the coiled-coil peptides during RPLC runs. N refers to the native state, I_F the free intermediate state and I_B the bound intermediate state.

dependency is eliminated. Here, our working hypothesis is that, just like the non-crosslinked coiled-coils, the crosslinked coiled-coil peptide will bind to the stationary phase matrix as an extended single-stranded α -helix (Fig. 1). However, since the cross-linked coiled-coil is much more stable than non-crosslinked ones [26], conformation of the cross-linked coiled-coil in the mobile phase upon elution may be one of three possibilities depending on temperature: 100% coiled-coil, mixture of coiled-coil and single-stranded α -helix or 100% single-stranded α -helix. Low temperature will favor the coiled-coil conformation in the mobile phase, whilst high temperature will favor the single-stranded α -helical conformation.

3.2. Design of model synthetic peptides

The purpose of this study was to investigate the

stability of coiled-coil peptides in the N→I transition by RPLC and then compare this stability with the one determined in the N→D transition by calorimetry. More precisely, one needs to obtain the stability order of a few closely related analogs in the N→I transition and then compare this order with that in the N→D transition. In analytical RPLC, the observable parameter is retention time, t_R , which, under given stationary phase and mobile phase and running conditions, is a function of multiple variables, i.e., amino acid composition, polypeptide chain length, conformation, amphipathicity, neighboring residue pairs, etc. [27–30]. Since we are using t_R as a measure of stability, it is necessary to design a series of peptides which have different stabilities but are otherwise identical in terms of amino acid composition, chain length, helicity, amphipathicity, neighboring residue pairs, etc. In other words, the stability difference among the peptides should be due to residue interactions in the tertiary/quaternary structure. Only then, can one conclude that retention time differences are due to intrinsic stability differences of the coiled-coils rather than caused by differences in their interaction with the stationary and mobile phases during RPLC. To this end, we adopted a novel sequence variation method called residue shuffling, which permutes guest residues in a symmetric sequence frame with equivalent host sites (Fig. 2). Permutation of guest residues at equivalent host sites has the benefit that factors other than interactions between the guest residues are conserved among the analogs. Previous research has shown that residue shuffling is very effective in isolating a single factor and gauging its contribution to protein stability [31,32].

The sequences of four peptides generated by residue shuffling, $\alpha\alpha$ -36, $\beta\beta$ -36, $\alpha\beta$ -36 and $\gamma\delta$ -36 are shown in Fig. 2. All the peptides are made of two chains, each of 36 residues, crosslinked by a disulfide bond near the N-terminal. All the peptide analogs have identical amino acid composition, amphipathicity, chain length and charge density, and all the guest residues have identical neighboring pairs. The only difference is the packing arrangement of hydrophobic core residues.

Peptide retention time is monitored as a function of temperature. Temperature, in the absence of any structural changes, will affect the equilibrium dis-

Peptides	Sequences
host	$1 \quad a \quad d \quad a_{10} \quad d_{13} \quad a \quad d \quad a_{24} \quad d_{27} \quad a \quad d \quad 36$ $\text{YEC} \text{E} \text{L} \text{E} \text{K} \text{E} \text{X} \text{E} \text{E} \text{X} \text{E} \text{K} \text{E} \text{K} \text{E} \text{E} \text{K} \text{E} \text{K} \text{E} \text{X} \text{E} \text{E} \text{X} \text{E} \text{K} \text{E} \text{L} \text{E} \text{E} \text{V} \text{E} \text{Y} \text{-amide}$
$\alpha\alpha$ -36	$\alpha: \text{YEC} \text{E} \text{L} \text{E} \text{K} \text{E} \text{L} \text{E} \text{E} \text{L} \text{E} \text{K} \text{E} \text{K} \text{E} \text{E} \text{K} \text{E} \text{L} \text{E} \text{E} \text{L} \text{E} \text{K} \text{E} \text{L} \text{E} \text{E} \text{V} \text{E} \text{Y} \text{-amide}$ $\alpha: \text{YEC} \text{E} \text{L} \text{E} \text{K} \text{E} \text{L} \text{E} \text{E} \text{L} \text{E} \text{K} \text{E} \text{K} \text{E} \text{E} \text{K} \text{E} \text{L} \text{E} \text{E} \text{L} \text{E} \text{K} \text{E} \text{L} \text{E} \text{E} \text{V} \text{E} \text{Y} \text{-amide}$
$\beta\beta$ -36	$\beta: \text{YEC} \text{E} \text{L} \text{E} \text{K} \text{E} \text{L} \text{E} \text{E} \text{V} \text{E} \text{K} \text{E} \text{K} \text{E} \text{E} \text{K} \text{E} \text{L} \text{E} \text{E} \text{V} \text{E} \text{K} \text{E} \text{L} \text{E} \text{E} \text{V} \text{E} \text{Y} \text{-amide}$ $\beta: \text{YEC} \text{E} \text{L} \text{E} \text{K} \text{E} \text{L} \text{E} \text{E} \text{V} \text{E} \text{K} \text{E} \text{K} \text{E} \text{E} \text{K} \text{E} \text{L} \text{E} \text{E} \text{V} \text{E} \text{K} \text{E} \text{L} \text{E} \text{E} \text{V} \text{E} \text{Y} \text{-amide}$
$\alpha\beta$ -36	$\alpha: \text{YEC} \text{E} \text{L} \text{E} \text{K} \text{E} \text{L} \text{E} \text{E} \text{L} \text{E} \text{K} \text{E} \text{K} \text{E} \text{E} \text{K} \text{E} \text{L} \text{E} \text{E} \text{L} \text{E} \text{K} \text{E} \text{L} \text{E} \text{E} \text{V} \text{E} \text{Y} \text{-amide}$ $\beta: \text{YEC} \text{E} \text{L} \text{E} \text{K} \text{E} \text{L} \text{E} \text{E} \text{L} \text{E} \text{K} \text{E} \text{K} \text{E} \text{E} \text{K} \text{E} \text{L} \text{E} \text{E} \text{L} \text{E} \text{K} \text{E} \text{L} \text{E} \text{E} \text{V} \text{E} \text{Y} \text{-amide}$
$\gamma\delta$ -36	$\gamma: \text{YEC} \text{E} \text{L} \text{E} \text{K} \text{E} \text{L} \text{E} \text{E} \text{V} \text{E} \text{K} \text{E} \text{K} \text{E} \text{E} \text{K} \text{E} \text{L} \text{E} \text{E} \text{V} \text{E} \text{K} \text{E} \text{L} \text{E} \text{E} \text{V} \text{E} \text{Y} \text{-amide}$ $\delta: \text{YEC} \text{E} \text{L} \text{E} \text{K} \text{E} \text{L} \text{E} \text{E} \text{L} \text{E} \text{K} \text{E} \text{K} \text{E} \text{E} \text{K} \text{E} \text{L} \text{E} \text{E} \text{L} \text{E} \text{K} \text{E} \text{L} \text{E} \text{E} \text{V} \text{E} \text{Y} \text{-amide}$
$\omega\omega$ -36	$\omega: \text{YEC} \text{E} \text{L} \text{E} \text{K} \text{E} \text{L} \text{E} \text{E} \text{V} \text{E} \text{K} \text{E} \text{K} \text{E} \text{E} \text{K} \text{E} \text{L} \text{E} \text{E} \text{L} \text{E} \text{K} \text{E} \text{L} \text{E} \text{E} \text{V} \text{E} \text{Y} \text{-amide}$ $\omega: \text{YEC} \text{E} \text{L} \text{E} \text{K} \text{E} \text{L} \text{E} \text{E} \text{V} \text{E} \text{K} \text{E} \text{K} \text{E} \text{E} \text{K} \text{E} \text{L} \text{E} \text{E} \text{L} \text{E} \text{K} \text{E} \text{L} \text{E} \text{E} \text{V} \text{E} \text{Y} \text{-amide}$ $1 \quad a \quad d \quad a_{10} \quad d_{13} \quad a \quad d \quad a_{24} \quad d_{27} \quad a \quad d \quad 36$
A18	Ac-EAEKAAKEAEKAAKEAEK-amide
RC30	Ac-(GKGLG) ₆ -amide
RC11	Ac-KYGLGGAGGLK-amide

Fig. 2. Peptide sequences. The host frame sequence has translational invariant symmetry because the guest sites, indicated by X, have identical neighboring residue pairs. Five peptides, $\alpha\alpha$ -36, $\beta\beta$ -36, $\alpha\beta$ -36, $\gamma\delta$ -36 and $\omega\omega$ -36 are generated by shuffling hydrophobic core guest residues, Val and Leu, in a host frame at positions a_{10} , d_{13} , a_{24} and d_{27} as indicated. In peptide $\omega\omega$ -36, all the α -Glu (E) residues are replaced by γ -Glu (ϵ), which prevents the formation of α -helical structure. Each of the five peptides is made of two polypeptide chains crosslinked by a disulfide bond at position 3 from the N-terminus. There are five individual chains, α , β , γ , δ , ω , all of which consist of 36 residues. A18 is a non-associating amphipathic α -helical peptide of 18 residues, while RC11 and RC30 are two random coil peptides, of 11 and 30 residues, respectively. Ac- and -amide denote N-terminal acetylation and C-terminal amidation, respectively.

tribution constant of a peptide between the mobile and the stationary phase, the viscosity constant, diffusion rate, etc. [33–35]. In order to account for these effects, it is necessary to have a peptide which is a random coil but otherwise identical to the four coiled-coil peptides. Then, the retention time difference between any given peptide and its random coil

counterpart is purely a conformational effect. Since both the organic co-solvent (typically acetonitrile) and the stationary phase ligands in RPLC can induce helical conformation among amphipathic peptides, this reference peptide should remain a random coil in the presence of strong helix-inducing reagents, such as 2,2,2-trifluoroethanol (TFE) or acetonitrile. In other words, this control peptide should have no intrinsic helix-forming capability. This is achieved by substituting all the α -Glu (E) residues in the host frame with γ -Glu (ϵ) residues, i.e., the carboxyl group of the Glu residues involved in peptide bond formation has been switched from the α -carboxyl group to the side chain γ -carboxyl group. Since two extra methylene groups are thus added to the polypeptide backbone at every second position, this should abolish the intrinsic helix-forming capability by violating the backbone geometric requirement of hydrogen bonding. The sequence of this peptide, $\omega\omega$ -36, is shown in Fig. 2.

Reduced and carboxamidomethylated (to prevent air oxidation of the cysteine residues and the formation of an interchain disulfide bond) single-stranded poly-peptides with identical amino acid composition were also prepared (α 36-CM, β 36-CM and ω 36-CM). These peptides serve to illustrate the difference in retention behavior between non-crosslinked and crosslinked amphipathic peptides. Also included in the study was a short, 18-residue amphipathic helical peptide, A18, (in previous work, this peptide was referred to as AA9 [36,37]), and two random coil peptides, RC11 and RC30 of 11 and 30 residues, respectively (Fig. 2). These peptides serve as controls to ascertain that, during RPLC runs, the tertiary/quaternary structure was indeed disrupted but not the secondary structure.

3.3. Conformation of the peptides in the mobile phase and their stability in the $N \rightarrow D$ transition

Since typical reversed-phase runs of peptides are performed at pH 2.0 with an initial aqueous eluent, all structural and thermodynamic characterizations of the peptides were carried out at pH 2.0 in aqueous solution. Fig. 3A gives the CD spectra of peptides $\alpha\alpha$ -36, $\beta\beta$ -36, $\alpha\beta$ -36 and $\gamma\delta$ -36. Within experimental error, these four peptides have identical spectra

and molar ellipticities indicative of the formation of a fully folded α -helical coiled-coil. Sedimentation equilibrium analysis shows that all the crosslinked peptides exist as disulfide-bridged two-stranded monomers. Differential scanning calorimetric measurements demonstrate that all four peptides are denatured in a two-state fashion [32]. The combined results of CD spectroscopy, analytical ultracentrifugation and calorimetry confirm that all four crosslinked peptides form two-stranded α -helical coiled-coils of identical helical content and unfold as single cooperative units. This forms the basis of a meaningful comparison of their physical-chemical properties. Although identical otherwise, variation in the arrangements of hydrophobic core residues caused marked differences in structural stability among the four coiled-coil peptides. The order of stability of the four peptides in the $N \rightarrow D$ transition measured by calorimetry is: $\alpha\beta$ -36 (86.8°C) < $\beta\beta$ -36 (89.8°C) < $\gamma\delta$ -36 (94.0°C) < $\alpha\alpha$ -36 (98.9°C) with the transition temperature, T_i , shown in the parentheses [32].

Fig. 3B shows the CD spectra of peptide $\omega\omega$ -36 with and without 50% TFE. As expected, this peptide is a random coil and cannot be induced into an α -helical structure by TFE which means that it has indeed lost its intrinsic capability of forming an α -helix. The CD spectra of non-crosslinked peptides α 36-CM and β 36-CM in aqueous buffer at pH 2.0 are shown in Fig. 3B and indicate that both peptides are fully folded α -helical peptides. Previous studies have shown that peptide A18 is helical but peptides RC11 and RC30 are random coils [36,37]. The effect of the mobile phase co-solvent, acetonitrile, on the conformation of the coiled-coil peptide is demonstrated in Fig. 3C and D, which show the CD spectra of the most stable coiled-coil peptide, $\alpha\alpha$ -36, in the absence and the presence of 35% (v/v) acetonitrile at 5°C and 80°C, respectively.

Molecular masses of the both non-crosslinked peptides (8750 and 8900 for α 36-CM and β 36-CM, respectively), determined by analytical ultracentrifugation (Fig. 4), are within 5% of dimer molecular masses (9210). Combining the results of CD spectroscopy and analytical ultracentrifugation, it is clear that both α 36-CM and β 36-CM form two-stranded α -helical coiled-coils in pH 2.0 aqueous buffer at low temperatures. The fact that the average molecular mass of β 36-CM at is 8900 at 5°C but 7640 at

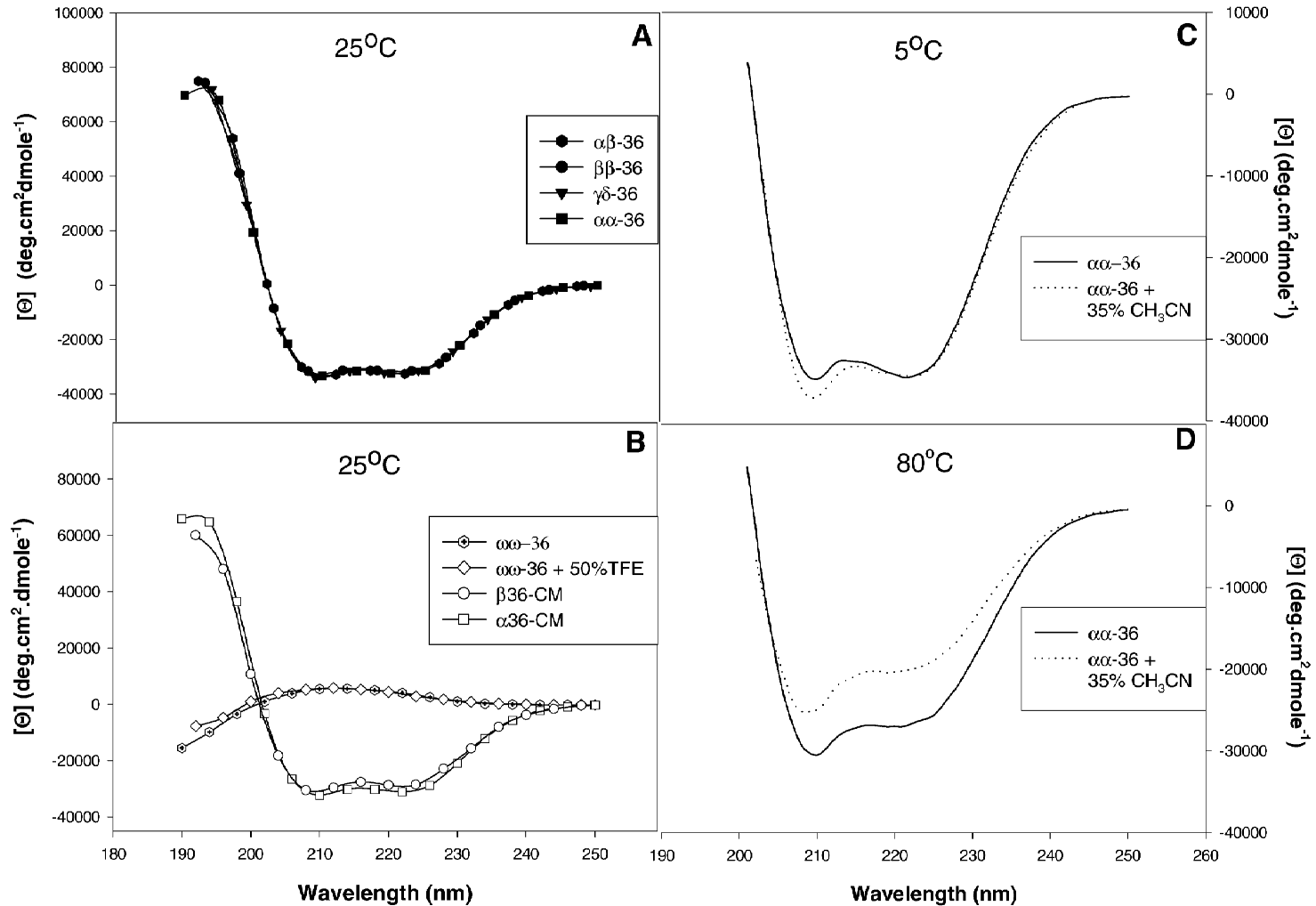


Fig. 3. Circular dichroism (CD) spectra of the various peptides at pH 2.0. The solution is buffered by 25 mM phosphoric acid with no added salt. (A) CD spectra of the disulfide bridged two-stranded α -helical coiled-coils at 25°C. (B) CD spectra of the random coil peptide $\omega\omega$ -36 without TFE and with 50% TFE in the buffer. Also shown in (B) are the CD spectra of the reduced and carboxamidomethylated single-stranded α -helical peptides α 36-CM and β 36-CM. Carboxamidomethylation by iodoacetamide of reduced peptides prevents air oxidation of cysteine residues and formation of the disulfide bond. (C and D) CD spectra of peptide $\alpha\alpha$ -36 in the absence and presence of 35% acetonitrile at 5°C and 80°C, respectively.

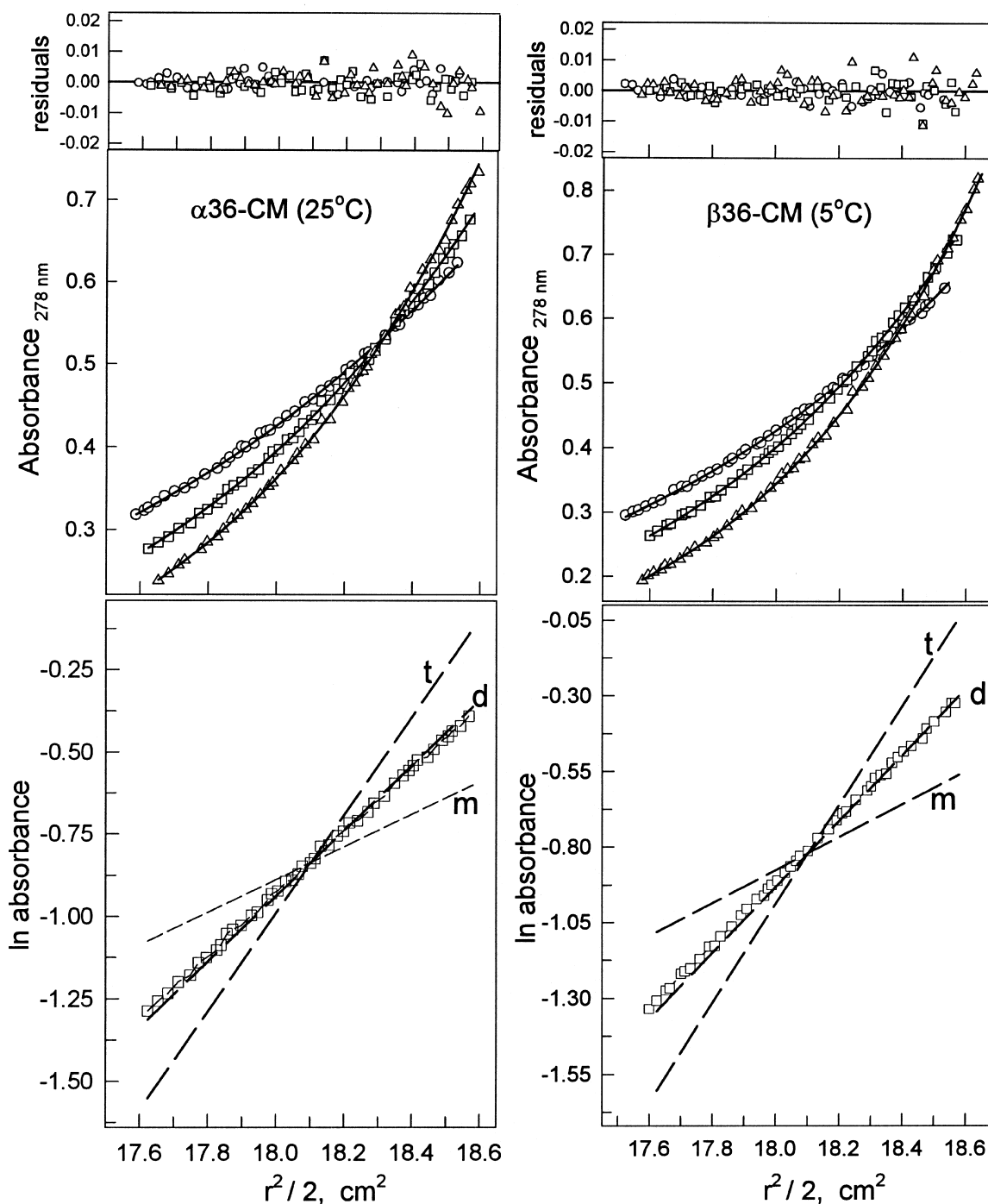


Fig. 4. Sedimentation equilibrium analysis of the molecular mass of the two carboxamidomethylated peptides, $\alpha 36\text{-CM}$ at 25°C (left panels) and $\beta 36\text{-CM}$ at 5°C (right panels). The same analysis was also performed for $\beta 36\text{-CM}$ at 25°C (data not shown). Runs are performed at three speeds: 26 000 (Δ), 30 000 (\square) and 34 000 rpm (\circ). The middle panels show the fitting results of a single-species model at all three different speeds. The top panels show the residuals of the fit. For $\alpha 36\text{-CM}$, the fittings give a molecular mass of 8750 at 25°C . For $\beta 36\text{-CM}$, the fittings give a molecular mass of 8900 at 5°C and 7640 at 25°C . The lower panels show a plot of \ln absorbance versus $r^2/2$ and compare the fitting to monomer (m), dimer (d) and trimer (t). The monomer, dimer and trimer molecular masses are 4607, 9214 and 13 821, respectively.

25°C is consistent with a temperature induced shift in the dimer-monomer equilibrium to an increased concentration of monomer. Upon elution, the non-crosslinked peptides will exist as monomeric helices due to a combined effect of low peptide concentration and presence of acetonitrile, as demonstrated in previous studies [5–7].

3.4. Retention behavior of random coil and non-crosslinked amphipathic peptides

Fig. 5A shows the plots of the retention times of α 36-CM, β 36-CM, ω 36-CM and $\omega\omega$ -36 versus temperature. It is clear within the entire experimental temperature range that the amphipathic peptides

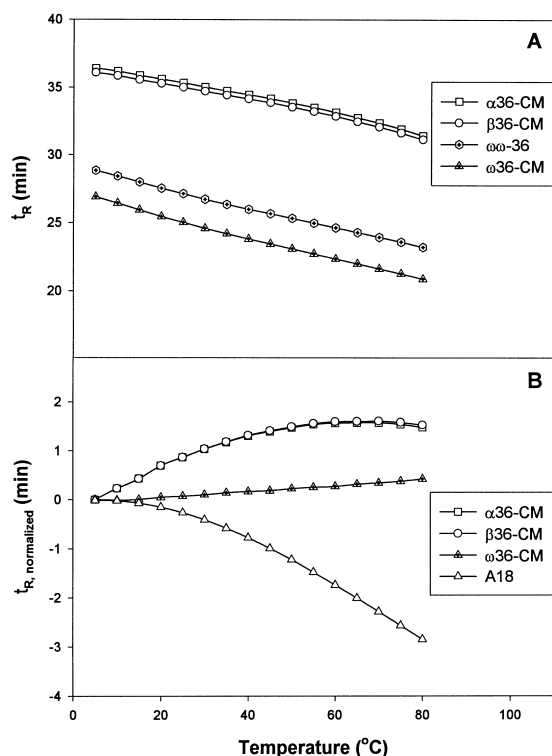


Fig. 5. Contrast of the retention behavior of amphipathic peptides and random coil peptides. (A). Comparison of the corrected retention time, t_R , of single-stranded amphipathic peptides with random coil peptides of identical hydrophobicity. (B) Normalized retention time, $t_{R, \text{normalized}}$, of the short amphipathic peptide A18, the long amphipathic peptides α 36-CM, β 36-CM, and the random coil peptide ω 36-CM. $t_{R, \text{normalized}} = [t_R(\text{peptide}, \text{Temp.}) - t_R(\text{peptide}, 5^\circ\text{C})] - [t_R(\text{RC11}, \text{Temp.}) - t_R(\text{RC11}, 5^\circ\text{C})]$.

(α 36-CM and β 36-CM) are much more retentive than their random coil counterpart (ω 36-CM). In fact, α 36-CM, β 36-CM are more retentive than $\omega\omega$ -36, a peptide twice the size and containing twice as many of the same hydrophobic residues. Clearly, the amphipathic peptides have preferred binding domains due to α -helix formation compared to non-amphipathic random peptides. This confirms previous findings that amphipathic peptides bind to the stationary phase ligands as helices to maximize interaction between its non-polar face and the stationary phase [5–12]. The second feature of the retention behavior of these non-crosslinked peptides is that they are essentially parallel to that of the random coil peptides. Since the random coil peptides undergo no conformational changes in either the mobile phase or the stationary phase, this parallel behavior of the non-crosslinked peptides indicates a lack of conformational transition for these peptides throughout the experimental temperature range. Fig. 5B shows plots of the normalized retention time, $t_{R, \text{normalized}}$, of α 36-CM, β 36-CM, ω 36-CM and A18 versus temperature. As can be seen, sharp differences in retention behavior exist not only between the amphipathic peptides and the random coil peptide, but also between the larger and more hydrophobic amphipathic peptides (α 36-CM and β 36-CM) and the smaller and less hydrophobic amphipathic peptide (A18). Compared to the random coil, $t_{R, \text{normalized}}$, of A18 drops more precipitously as temperature increases, indicating that its helical structure is unraveling. From Fig. 5A and B, it is clear that the 36-residue amphipathic, peptides with a very strong hydrophobic apolar face or preferred binding domain (consisting of Leu and Val), bind to the stationary phase as helices up to a temperature of 80°C. As noted previously, the non-crosslinked peptides exist as single-stranded helices upon elution due to the combined effect of low peptide concentration and presence of acetonitrile.

3.5. RPLC behavior of the two-stranded coiled-coil peptides

Fig. 6 shows the RPLC chromatograms of the four coiled-coil peptides at 5°C and 80°C while Fig. 7A plots the retention times of all of the two-stranded

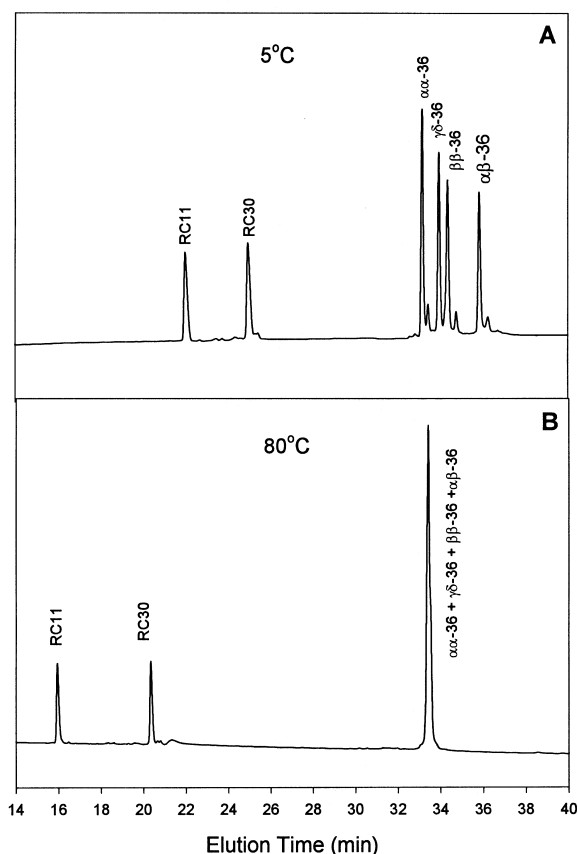


Fig. 6. Reversed-phase HPLC chromatograms of the four cross-linked α -helical coiled-coils and two random coil peptides, RC11 and RC30, at 5°C (panel A) and 80°C (panel B). Run conditions: linear A-B gradient (1%/min) at a flow-rate of 0.4 ml/min, where solvent A is 0.05% TFA in water and solvent B is 0.05% TFA in acetonitrile. Column and instrument are described in the Experimental section.

peptides. As can be seen, the four crosslinked peptides were eluted separately at 5°C even though they have the same conformation. Their separation decreases with increasing temperature and at 80°C, the four peptides are co-eluted. Fig. 7B plots the corrected retention time, defined as $t_{R, \text{corrected}} = t_R(\text{peptide}) - t_R(\text{random coil})$, of the four coiled-coil peptides versus temperature. Since the contribution from the same hydrophobic side chains in the random coil conformation has already been subtracted out, $t_{R, \text{corrected}}$ contains structural information of the peptide during RPLC, in both the mobile phase and the stationary phase. Structural features of these peptides in the stationary phase are reflected by

$t_{R, \text{corrected}} > 0$, indicating that the coiled-coil peptides are more retentive than their random coil counterpart. The reason that $t_{R, \text{corrected}} > 0$ reflects structural features of peptide on the stationary phase rather than in the mobile phase is because hydrophobic side chains in a coiled-coil are much more shielded in the mobile phase than those in a random coil. This would make the coiled-coils less, rather than more, retentive than the random coil. Thus, the only explanation for the coiled-coils being more retentive is that they interact preferentially with the stationary phase, i.e., the constituent amphipathic helices of the coiled-coil peptides bind to the stationary phase ligands as extended α -helices. Structural features of these peptides in the mobile phase are reflected by $dt_{R, \text{corrected}}/dT > 0$, i.e., $t_{R, \text{corrected}}$ of the coiled-coils climbs steadily with increasing temperature. This is in sharp contrast with the non-crosslinked peptides whose retention times run almost parallel with those of the random coil peptides as temperature increases (compare Fig. 5A and Fig. 7A). Clearly, the $N \leftrightarrow I$ equilibrium in the mobile phase is pushed toward the I state by increasing temperature, making the hydrophobic side chains more exposed and therefore more accessible to stationary phase ligands. The extent of shielding vs. exposure of hydrophobic side chains (N vs. I), in the temperature range 5°C–80°C, can be assessed by comparing the retention behavior of the crosslinked and the non-crosslinked peptides. Fig. 7C shows that the crosslinked homo-stranded peptides ($\alpha\alpha$ -36 and $\beta\beta$ -36) are less retentive at low temperature than their non-crosslinked counterparts (α 36-CM and β 36-CM) even though the crosslinked ones have twice as many of the same hydrophobic residues and identical amphipathicity as the non-crosslinked ones. On the other hand, as temperature increases, the crosslinked peptides eventually become more retentive than the non-crosslinked ones. The implication is that in the mobile phase during elution, the crosslinked peptides exist predominantly as coiled-coils at 5°C but become predominantly extended single-stranded α -helices at 80°C. This conclusion of the status of the crosslinked peptides is corroborated by CD spectra of $\alpha\alpha$ -36 at 5°C and 80°C, with and without 35% acetonitrile (Fig. 3C and D). The concentration of acetonitrile at which $\alpha\alpha$ -36 was eluted is 35% and, therefore, 0% and 35% acetonitrile represent the two limiting values of the mobile phase solvent composition. At 5°C,

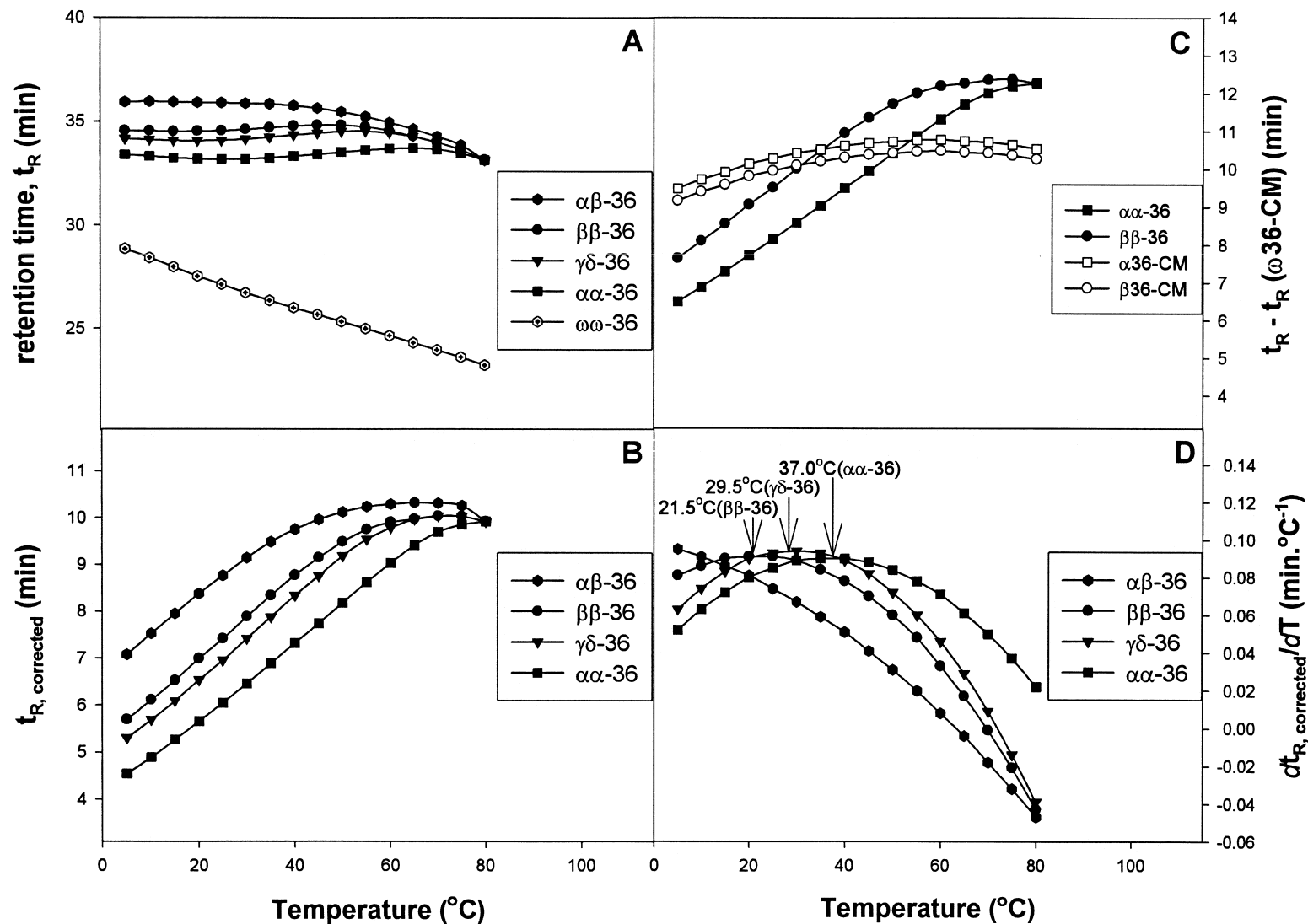


Fig. 7. Retention behavior of the crosslinked two-stranded α -helical coiled-coils as a function of temperature. (A) Retention times of peptides (t_R) vs. temperature. (B) Corrected retention times ($t_{R,corrected}$) vs. temperature for the four crosslinked coiled-coil peptides. $t_{R,corrected}(\text{peptide}) = t_R(\text{peptide}) - t_R(\text{random coil}, \omega\omega\text{-}36)$. (C) Comparison of the retention times of the homo-stranded crosslinked coiled-coil peptides ($\alpha\alpha$ -36 and $\beta\beta$ -36) with their non-crosslinked counterparts ($\alpha 36$ -CM and $\beta 36$ -CM) after correcting for the same random coil standard ($\omega 36$ -CM). (D) First derivative of $t_{R,corrected}$ vs. temperature. The temperature at which $dt_{R,corrected}/dT$ reaches maximum is 37.0°C, 29.5°C and 21.5°C for $\alpha\alpha$ -36, $\gamma\delta$ -36, $\beta\beta$ -36, respectively. For $\alpha\beta$ -36, this temperature lies outside the lower limit of the experimental temperature range.

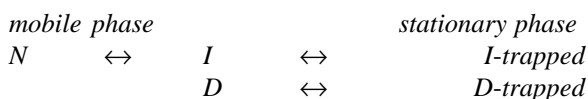
acetonitrile has little effect on the molar ellipticity (Θ) except changing the ratio of $\Theta_{222}/\Theta_{208}$ from slightly above 1.0 to slightly below 1.0. At 80°C, the ellipticity of $\alpha\alpha$ -36 is reduced as a result of elevated temperature, with or without 35% acetonitrile, but to a much greater extent with 35% acetonitrile. This greater reduction in helicity in the presence of 35% acetonitrile indicates a loss of interchain stabilization as a result of N→I transition facilitated by high temperature and acetonitrile. In other words, at 80°C, the peptide was largely an extended single-stranded α -helix in the mobile phase upon elution.

The above conclusion regarding the structural status of the crosslinked peptides explains why they are well separated at 5°C but are co-eluted at 80°C. At 5°C, with the coiled-coil conformation largely intact in the mobile phase, stability differences among the peptides caused by different arrangements of guest residues dictates that the more stable coiled-coil will have a larger fraction of its population in the N state compared to the less stable ones. This leads to less exposure of the hydrophobic side chains of the more stable coiled-coils (lower fraction of the open form I state) and consequently they are less retentive. On the other hand, at 80°C, the interchain interactions between the guest residues, the only source of difference among the crosslinked peptides, are not possible since the two helices are 100% in the open form, or I state. Consequently, these peptides have identical retention behavior because the extended helices of the I state have identical hydrophobicity and other properties. Accordingly, the transition temperature for the N→I process, $T_t(N\rightarrow I)$, must lie between 5°C and 80°C. This temperature can be determined by locating the position of maximum change of $t_{R, corrected}$, i.e., where $dt_{R, corrected}/dT$ reaches a maximum (Fig. 7D). $T_t(N\rightarrow I)$ for the fourth peptide, $\alpha\beta$ -36, lies outside the lower limit of the experimental temperature range. Three features of these $T_t(N\rightarrow I)$ values are worth noticing: (1) $T_t(N\rightarrow I)$ are lower than $T_t(N\rightarrow D)$ measured by calorimetry, which is expected. (2) Due to symmetry considerations [32], $T_t(N\rightarrow D)$ of $\gamma\delta$ -36 (94.0°C) is the average of $\alpha\alpha$ -36 (98.9°C) and $\beta\beta$ -36 (89.8°C). This relationship is also satisfied by the $T_t(N\rightarrow I)$ values where $\gamma\delta$ -36 (29.5°C) is the average of $\alpha\alpha$ -36 (37.0°C) and $\beta\beta$ -36 (21.5°C). (3) Peptide $\alpha\beta$ -36, the least stable of the

four crosslinked peptides in the N→I transition, is the only one which involves potential clashes between guest leucine side chains [32]. Peptide $\alpha\beta$ -36 also stands out in its RPLC retention behavior as the only one whose $T_t(N\rightarrow I)$ lies below experimental temperature range. The reason for this awaits further investigation.

3.6. Transition order parameter and phase diagram

Due to the high stability of the coiled-coil peptides used, RPLC is only able to monitor the N→I transition in this study. However, depending on the stability of the peptides, RPLC could be used to monitor other parts of the conformational transition. For coiled-coils in the general case, the distribution between the mobile phase and the stationary phase is determined by the following equilibria between the N, I and D states (stationary phase is denoted by italics):



The above analysis demonstrates that $t_{R, corrected} = t_R(\text{peptide}) - t_R(\text{random coil})$ is a very effective parameter in describing structural transitions during RPLC runs. This point is reinforced by comparing $t_{R, corrected}$ of the homo-stranded crosslinked peptides with their non-crosslinked counterparts (Fig. 8). As can be seen, $t_{R, corrected}$ of both the crosslinked peptides and their non-crosslinked counterparts are far from zero at any temperature. Furthermore, as temperature increases, $t_{R, corrected}$ of the crosslinked peptides increased closer to the level of the non-crosslinked ones, indicating that the coiled-coils are behaving more and more like single-stranded amphipathic peptides, apparently due to the thermally-induced increase in the fraction of the I state. The effectiveness of $t_{R, corrected}$ to describe structural transitions during RPLC comes from the fact that the contribution to retention time from hydrophobic side chains in the polypeptide chain in the random coil conformation has already been subtracted out. Therefore, $t_{R, corrected} = 0$ if the peptide is in the random coil conformation in both the stationary and the

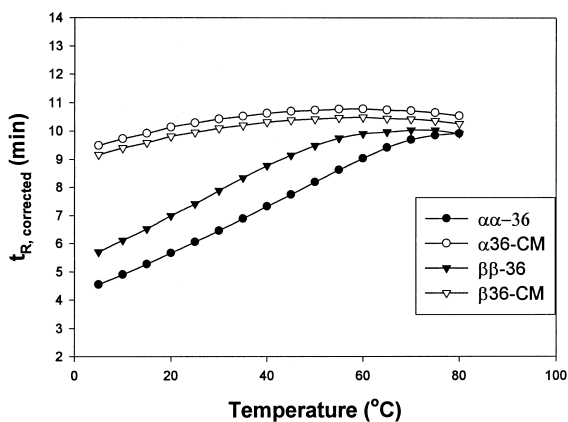


Fig. 8. $t_{R, \text{corrected}}$ as a structural transition order parameter. It shows that as temperature increases, the crosslinked ($\alpha\alpha$ -36 and $\beta\beta$ -36) and the non-crosslinked (α 36-CM and β 36-CM) peptides are behaving more and more alike.

mobile phase. Any deviation from zero is a purely conformational effect. In this sense, $t_{R, \text{corrected}}$ is analogous to the so-called order parameter used to describe macroscopic phase transitions, such as condensation and a plot of $t_{R, \text{corrected}}$ vs. temperature is analogous to a phase diagram [38]. Pursuing this analogy one step further, the temperature at which $t_{R, \text{corrected}}=0$ would be analogous to the critical temperature T_c . Extrapolating experimental data from Fig. 8, a hypothetical phase diagram is shown in Fig. 9.

3.7. Folding mechanism of crosslinked coiled-coils

In this work, we trapped the monomeric α -helical state of coiled-coils, which is a structural intermediate state between fully folded coiled-coil and the unfolded polypeptide chain. A recent kinetic study demonstrated that crosslinked coiled-coils fold along a single robust pathway [39]. Therefore, it is legitimate to ask if this structural intermediate state is also a kinetic intermediate which is an essential step on the folding pathway. This is answered by comparing the stability order of these coiled-coils in the $N \rightarrow I$ transition with that in the $N \rightarrow D$ transition. If the monomeric α -helical state is an on-pathway intermediate, then its stability should be proportional to the stability of the coiled-coil state. Therefore, the stability order of these closely related coiled-coils in

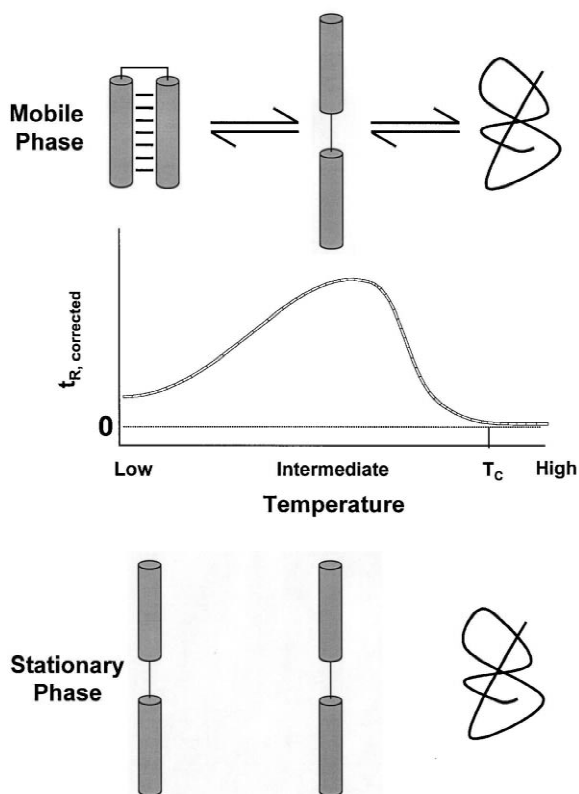


Fig. 9. A hypothetical phase diagram for crosslinked coiled-coils based on extrapolation of the retention behavior of coiled-coils used in this work. $t_{R, \text{corrected}}$ line is the co-existence line above which the peptide will be in the mobile phase and below which the peptide will be bound to the stationary phase. The value of $t_{R, \text{corrected}}$ is determined by the extent to which the peptide structure deviates from the random coil conformation. The structural status of the peptides in the mobile and stationary phase are shown schematically above and below the co-existence line. T_c is the temperature above which $t_{R, \text{corrected}}=0$.

the $N \rightarrow I$ transition should be the same with that in the $N \rightarrow D$ transition. On the other hand, if the monomeric α -helical state is an off-pathway intermediate which either only exists under artificial conditions or acts as a kinetic trap, then there would be no simple correlation between the stability order of these coiled-coils in the $N \rightarrow I$ transition and that in the $N \rightarrow D$ transition. In this case, both the elution order and the transition temperature [$T_t(N \rightarrow I)$] provide the order of stability of the peptides in the $N \rightarrow I$ transition as $\alpha\beta$ -36 < $\beta\beta$ -36 < $\gamma\delta$ -36 < $\alpha\alpha$ -36 which is the same order as in the $N \rightarrow D$ transition as

determined by calorimetry. This agreement between these two stability orders is consistent with the monomeric α -helical state being not only a structural intermediate, but also a kinetic intermediate. However, the question whether the kinetic intermediate involves complete helix formation or partial helix formation only cannot be answered by this study because both scenarios are consistent with our results. This is because, due to the repetitiveness of coiled-coils sequences, if helix A is more stable than helix B, then part of A is still more stable than B. However, this uncertainty does not affect our main conclusion, which is that the coiled-coils fold through a hierarchical mechanism in which secondary structure formation precedes formation of tertiary/quaternary structure [1,2]. The same conclusion was reached for the folding of the GCN4-p1 coiled-coil from kinetic considerations based on the diffusion-collision model [40] and mutational studies [41].

4. Conclusions

This work demonstrates that reversed-phase liquid chromatography can trap amphipathic peptides in the helical conformation and hence provides an excellent tool to study the transition from the native state to the intermediate state for proteins whose secondary structure is comprised entirely of amphipathic helices. Applying this technique to a set of coiled-coil peptides of differing stability but identical in all other aspects, it was shown that the more stable a coiled-coil, the less retentive it is in reversed-phase liquid chromatography. Furthermore, the stability of coiled-coil peptides in the transition from the native to the intermediate state correlates with their stability in the transition from the native to the denatured state. From this, it is concluded that these crosslinked coiled-coils fold through a hierarchical mechanism in which the formation of at least part of the native secondary structure precedes the formation of the final coiled-coil structure.

Acknowledgements

We thank Paul Semchuck, Bob Luty and Les

Hicks for technical assistance. This work was supported by Medical Research Council of Canada Group in Protein Structure and Function and the Government of Canada's Network of Centres of Excellence program supported by the Medical Research Council of Canada and the National Science and Engineering Research Council through PENCE Inc. (the Protein Engineering Network of Centres of Excellence).

References

- [1] R.L. Baldwin, G.D. Rose, *Trends Biochem. Sci.* 24 (1999) 26.
- [2] R.L. Baldwin, G.D. Rose, *Trends Biochem. Sci.* 24 (1999) 77.
- [3] M.-H. Hao, H.A. Scheraga, *Acct. Chem. Res.* 31 (1998) 433.
- [4] K.A. Dill, *Protein Sci.* 8 (1999) 1166.
- [5] S.Y.M. Lau, A.K. Taneja, R.S. Hodges, *J. Chromatogr.* 317 (1984) 129.
- [6] S.Y.M. Lau, A.K. Taneja, R.S. Hodges, *J. Biol. Chem.* 259 (1984) 13253.
- [7] N.E. Zhou, C.T. Mant, R.S. Hodges, *Pept. Res.* 3 (1990) 8.
- [8] R.A. Houghten, J.M. Ostresh, *Biochromatogr.* 2 (1987) 80.
- [9] V. Steiner, M. Scharr, K.O. Borsan, M. Mutter, *J. Chromatogr.* 586 (1991) 43.
- [10] A.W. Purcell, M.-I. Aguilar, R.E.H. Wettenhall, M.T. W Hearn, *Pept. Res.* 8 (1995) 160.
- [11] S.E. Blondelle, J.M. Ostresh, R.A. Houghten, E. Perez-Paya, *Biophys. J.* 68 (1995) 351.
- [12] D.S. Steer, P.E. Thompson, S.E. Blondelle, R.A. Houghten, M.-I. Aguilar, *J. Pept. Res.* 51 (1998) 401.
- [13] F.H.C. Crick, *Acta Crystallogr.* 6 (1953) 689.
- [14] E.K. O'Shea, J.D. Klemm, P.S. Kim, T. Alber, *Science* 254 (1991) 328.
- [15] R.S. Hodges, J. Sodek, L.B. Smillie, L. Jurasek, *Cold Spring Harbor Symp. Quart. Biol.* 37 (1972) 299.
- [16] R.S. Hodges, *Biochem. Cell. Biol.* 74 (1996) 133.
- [17] A. Lupas, *Trends Biochem. Sci.* 21 (1996) 375.
- [18] W.D. Kohn, C.T. Mant, R.S. Hodges, *J. Biol. Chem.* 272 (1997) 2583.
- [19] R.A. Kammerer, *Matrix Biol.* 15 (1997) 55.
- [20] W.D. Kohn, R.S. Hodges, *Trends Biotech.* 16 (1998) 379.
- [21] F. Rabanal, W.F. DeGrado, P.L. Dutton, *Tetrahedron Lett.* 37 (1996) 1347.
- [22] P.D. Semchuck, O.D. Monera, L.H. Kondejewski, C. Gannon, L. Danniels, I. Wilson, R.S. Hodges, in: P.T.P. Kaumaya, R.S. Hodges (Eds.), *Peptides: Chemistry, Structure and Biology*, Mayflower Scientific UK, UK, 1996, pp. 73–74.
- [23] I. Annis, B. Hargittai, G. Barany, *Methods Enzymol.* 289 (1997) 198.
- [24] K.C. Wagschal, B. Tripet, P. Lavigne, C.T. Mant, R.S. Hodges, *Protein Sci.* 8 (1999) 2312.

- [25] S.C. Gill, P.H. von Hippel, *Anal. Biochem.* 182 (1989) 319.
- [26] Y.B. Yu, P. Lavigne, C.M. Kay, R.S. Hodges, P.L. Privalov, *J. Phys. Chem., B* 103 (1999) 2270.
- [27] C.T. Mant, T.W.L. Lorne, J.A. Black, R.S. Hodges, *J. Chromatogr.* 458 (1988) 193.
- [28] C.T. Mant, N.E. Zhou, R.S. Hodges, *J. Chromatogr.* 476 (1989) 363.
- [29] R.S. Hodges, B.-Y. Zhu, N.E. Zhou, C.T. Mant, *J. Chromatogr. A* 676 (1994) 3.
- [30] T.J. Sereda, C.T. Mant, R.S. Hodges, *J. Chromatogr. A* 695 (1995) 205.
- [31] Y. Yu, O.D. Monera, R.S. Hodges, P.L. Privalov, *Biophys. Chem.* 59 (1996) 299.
- [32] Y.B. Yu, P. Lavigne, P.L. Privalov, R.S. Hodges, *J. Am. Chem. Soc.* 121 (1999) 8443.
- [33] R.H. Ingraham, S.Y.M. Lau, A.K. Taneja, R.S. Hodges, *J. Chromatogr.* 327 (1985) 77.
- [34] D. Guo, C.T. Mant, A.K. Taneja, R.S. Hodges, *J. Chromatogr.* 359 (1986) 519.
- [35] W.S. Hancock, D.R. Knighton, J.R. Napier, D.R. Harding, R. Venable, *J. Chromatogr.* 367 (1986) 1.
- [36] N.E. Zhou, C.M. Kay, B.D. Sykes, R.S. Hodges, *Biochemistry* 32 (1993) 6190.
- [37] T.J. Sereda, C.T. Mant, F.D. Sonnichsen, R.S. Hodges, *J. Chromatogr. A* 676 (1994) 139.
- [38] D.L. Goodstein, *States of Matter*, Dover, New York, 1996, Ch. 6.
- [39] L. Moran, J.P. Schneider, A. Kentsis, G.A. Reddy, T.R. Sosnick, *Pros. Natl. Acad. Sci. USA* 96 (1999) 10699.
- [40] J.K. Myers, T.G. Oas, *J. Mol. Biol.* 289 (1999) 205.
- [41] J.A. Zitzewitz, B. Ibarra-Molero, D.R. Fishel, K.L. Terry, C.R. Matthews, *J. Mol. Biol.* 296 (2000) 1105.